Multifunctional Products of Isoprene Oxidation in Polluted Atmosphere and Their Contribution to SOA

Xu, Z. N.

2021-01-16

Xu , Z N , Nie , W , Liu , Y L , Sun , P , Huang , D D , Yan , C , Krechmer , J , Ye , P L , Xu , Z , Qi , X M , Zhu , C J , Li , Y Y , Wang , T Y , Wang , L , Huang , X , Tang , R Z , Guo , S , Xiu , G L , Fu , Q Y , Worsnop , D , Chi , X G & Ding , A J 2021 , ' Multifunctional Products of Isoprene Oxidation in Polluted Atmosphere and Their Contribution to SOA ' , Geophysical Research Letters , vol. 48 , no. 1 , ARTN e2020GL089276 . https://doi.org/10.1029/2020GL089276

http://hdl.handle.net/10138/328445
https://doi.org/10.1029/2020GL089276

AGU ADVANCING EARTH AND SPACE SCIENCE

Geophysical Research Letters

RESEARCH LETTER
10.1029/2020GL089276

Multifunctional Products of Isoprene Oxidation in Polluted Atmosphere and Their Contribution to SOA

Z. N. Xu[1,2,3], W. Nie[1,2], Y. L. Liu[1,2], P. Sun[1], D. D. Huang[4], C. Yan[5], J. Krechmer[6], P. L. Ye[6], Z. Xu[1,2], X. M. Qi[1,2], C. J. Zhu[1,2], Y. Y. Li[1,2], T. Y. Wang[1,2], L. Wang[1,2], X. Huang[1,2], R. Z. Tang[7], S. Guo[7], G. L. Xiu[8], Q. Y. Fu[9], D. Worsnop[6], X. G. Chi[1,2], and A. J. Ding[1,2]

[1]Joint International Research Laboratory of Atmospheric and Earth System Sciences, School of Atmospheric Sciences, Nanjing University, Nanjing, China, [2]Jiangsu Provincial Collaborative Innovation Center of Climate Change, Nanjing, China, [3]College of Environmental & Resource Sciences, Zhejiang University, Zhejiang, China, [4]Shanghai Academy of Environmental Sciences, Shanghai, China, [5]Division of Atmospheric Sciences, Department of Physics, University of Helsinki, Helsinki, Finland, [6]Center for Aerosol and Cloud Chemistry, Aerodyne Research Inc., Billerica, MA, USA, [7]School of Environmental Science and Technology, Peking University, Beijing, China, [8]State Environmental Protection Key Lab of Environmental Risk Assessment and Control on Chemical Processes, School of Resources and Environmental Engineering, East China University of Science and Technology, Shanghai, China, [9]Shanghai Environmental Monitoring Center, Shanghai, China

Key Points:

- Simultaneous measurements of volatile organic compounds, highly functionalized intermediate compounds and organic aerosol were conducted
- Organic nitrates dominated the C4-C5 functionalized isoprene oxidation products detected by NO_3^- CIMS
- Most of the identified isoprene oxidation products were categorized as SVOC and can contributed to secondary organic aerosol

Supporting Information:

- Supporting Information S1

Correspondence to:
W. Nie,
niewei@nju.edu.cn

Citation:
Xu, Z. N., Nie, W., Liu, Y. L., Sun, P., Huang, D. D., Yan, C., et al. (2021). Multifunctional products of isoprene oxidation in polluted atmosphere and their contribution to SOA. *Geophysical Research Letters*, *48*, e2020GL089276. https://doi.org/10.1029/2020GL089276

Received 19 JUN 2020
Accepted 20 NOV 2020

Abstract Isoprene (2-methyl-1, 3-butadiene) is a nonmethane volatile organic compound (VOC) with the largest global emission and high reactivity. The oxidation of isoprene is crucial to atmospheric photochemistry and contributes significantly to the global formation of secondary organic aerosol. Here, we conducted comprehensive observations in polluted megacities of Nanjing and Shanghai during summer of 2018. We identified multiple functionalized isoprene oxidation products, of which 72% and 88% of the total mole concentration were nitrogen-containing species with the dominant compound being C5 dihydroxyl dinitrate ($C_5H_{10}N_2O_8$). We calculated the volatility using the group-contribution method and estimated the particle-phase concentration by equilibrium gas/particle partitioning. The results showed that the multifunctional products derived from isoprene oxidation can contribute to 2.6% of the total organic aerosol mass (0.28 ± 0.27 μg/m^3), highlighting the potential importance of isoprene oxidation in polluted regions.

Plain Language Summary Isoprene, as one of the most important precursors to form secondary organic aerosol (SOA) globally, has been extensively studied, most of which however focused in the pristine regions. In polluted urban areas, where isoprene would interact significantly with anthropogenic emissions, for example, NO_x, the understanding of SOA formation potential of isoprene is rather controversial. Here, we used state-of-the-art instruments to measure isoprene, highly functionalized intermediate compounds and organic aerosol simultaneously at two suburban sites in eastern China region and identify several tens of isoprene oxidation products with most of which identified as nitrogen-containing species, confirming the significant interaction between the isoprene derived peroxy radicals and NO_x. These multifunctional products are mostly semi-volatile species and can contribute considerably to the observed SOA, highlighting an important role of biogenic volatile organic compounds oxidation on SOA formation under high-NOx conditions, for example, anthropogenic emission dominant regions.

1. Introduction

Secondary organic aerosol (SOA) forms through the oxidation of various volatile organic compounds (VOCs) and consists of a large proportion of the total aerosol mass (Huang et al., 2014; Ng et al., 2010; Sun et al., 2013; Zhang et al., 2007; Zhang, Yee, et al., 2018). Isoprene (2-methyl-1, 3-butadiene), mainly originating from biogenic sources, has the largest emission of all nonmethane VOCs with a global emission of ~600 Tg C yr^{-1} (Guenther et al., 2006). Isoprene is highly reactive and can be readily oxidized by various oxidants (mainly OH, NO_3, and O_3) in the atmosphere, affecting the abundance of global SOA (Carlton et al., 2009; Claeys et al., 2004; Wennberg et al., 2018). The state-of-the-art isoprene oxidation mechanisms have been incorporated into the model to estimate global budget of isoprene SOA (Bates & Jacob, 2019; Müller et al., 2019; Pai et al., 2019; Stadtler et al., 2018) during recent years. Although significant progress

has been made on the isoprene oxidation scheme, uncertainties about isoprene oxidation under various polluted conditions still exist, which would affect the estimation of the isoprene SOA yield among polluted environments.

Isoprene oxidation and SOA contribution under NO_x free or low-NO_x condition ([NO_x]<1 ppb) have been well studied during past years (Kroll et al., 2006). The formation of dihydroxy epoxides (IEPOX) dominates the isoprene oxidation process (Paulot et al., 2009) at yields greater than 75% (Bates et al., 2014). The reactive uptake of IEPOX onto aerosol seeds has been confirmed to form SOA (D'Ambro et al., 2017; Lin et al., 2011; Liu et al., 2015; Nguyen et al., 2014; Xu et al., 2015; Zhang, Chen, et al., 2018). Aside from the IEPOX pathway, the multifunctional compounds formed through isoprene oxidation would be of low enough volatility to partition efficiently to the particle phase (Kroll & Seinfeld, 2008). Various studies have reported the formation mechanisms of multifunctional isoprene oxidation products and their contribution to SOA formation under low-NO conditions (Berndt et al., 2016; Krechmer et al., 2015; Riva et al., 2016; Wang et al., 2018), with SOA yield ranging from 5.8% to 11%.

Under polluted environments, the effect of NO_x on isoprene SOA formation has not yet been fully interpreted. A continuous increase in SOA was observed in isoprene-photooxidation with increased NO injection (Kroll et al., 2005; Nga et al., 2006). Multiple studies have indicated oppositely that the addition of NO will suppress SOA formation (D'Ambro et al., 2017; Kroll et al., 2008; Liu et al., 2016). Several other experiments have reported a nonlinear effect of NO_x (Dommen et al., 2006; Kroll et al., 2006; Xu et al., 2014). Field measurements have highlighted the importance of NO_x on isoprene SOA formation: the aircraft and ground observations indicated that SOA formation was enhanced when NO_x was mixed with isoprene-rich air masses (Setyan et al., 2012; Shilling et al., 2013).

The oxidation of methacryloyl peroxynitrate was considered to be the important SOA formation pathway under high-NO_x conditions (Chan et al., 2010; Kjaergaard et al., 2012; Lin et al., 2013; Nguyen et al., 2015; Schwantes et al., 2019; Surratt et al., 2009), but have also been pointed out to be suppressed under atmospheric humidity (Schwantes et al., 2019; Zhang et al., 2011). The equilibrium gas-particle partitioning of low volatility isoprene nitrates is believed to be another important source of isoprene SOA, although the yields of multifunctional isoprene nitrates have not been well studied (Lee et al., 2014; Wennberg et al., 2018). Schwantes et al. (2019) presented that the SOA yield from multifunctional organic nitrate was significantly higher than previously thought under high NO conditions (~15%). The observational evidence indicated that highly functionalized organic nitrates account for at least 58% of particulate nitrate and the diurnal profiles of C5 functionalized organic nitrates were consistent with isoprene (Lee et al., 2015).

In this work, we present the field measurements of organic aerosol (OA), gas-phase precursors (isoprene and its major oxidation products) and highly functionalized compounds during June 22 to 27 of 2018 in the Feng Xian campus of East China University of Science and Technology (ECUST), Shanghai and during July 13 to August 9 at the Station for Observation Regional Processes of the Earth System (SORPES) in the Xianlin campus of Nanjing University. Such comprehensive observation makes it possible to identify major highly functionalized isoprene oxidation products and to semi-quantify their contribution to SOA formation in the real atmosphere. The two observational sites are both located in the Yangtze River Delta (YRD), which are representative of the eastern China region.

2. Field Observations

2.1. Site Description

Comprehensive field observations were conducted during the summer of 2018 at two representational sites located in the YRD, eastern China region. The first site was the SORPES in the Xianlin campus of Nanjing University, which is the regional background station upwind of Nanjing downtown. The geographic location and meteorological characteristics were described in detail by Ding et al. (2013). The second site was located in the Fengxian campus of ECUST, which was ~50 km south of downtown Shanghai, near Hangzhou Bay, across from which the densest broad leaf forested area in China is located (Qi et al., 2019).

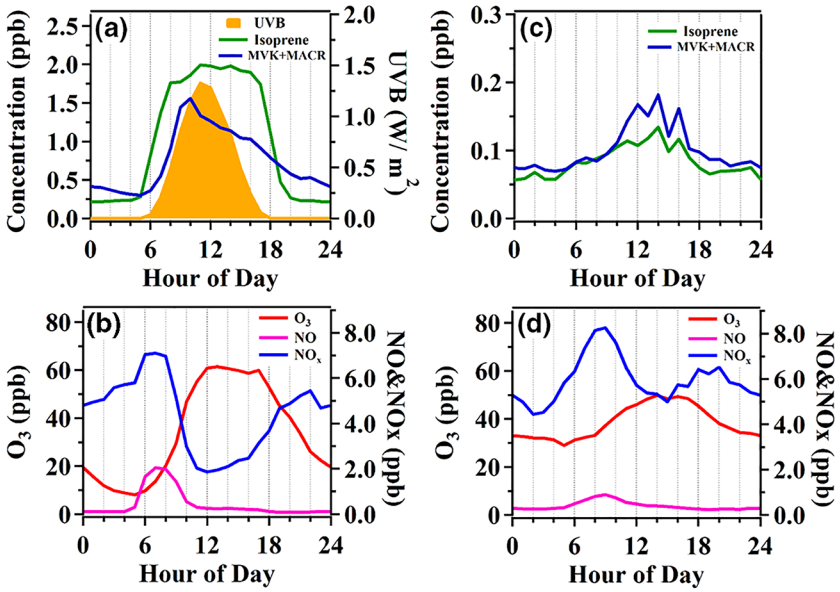

Figure 1. Diel pattern of gas-phase precursors in two sites: (a) and (b) SORPES (Nanjing); (c) and (d) ECUST (Shanghai). (a) and (c) isoprene and sum of methyl vinyl ketone (MVK) and methacrolein (MACR). UVB in Nanjing site is also included. (b) and (d) trace gases (O_3, NO, and NO_x).

2.2. Methodology

Measurements of highly oxidized gas-phase organic species were applied with an Aerodyne high-resolution time-of-flight chemical ionization mass spectrometer (CIMS; HR-ToF-CIMS or HR- CI-APi-TOF). In this work, the CIMS was equipped with an atmospheric pressure nitrate-ion (NO_3^-) ionization source (Airmodus Ltd.). The VOCs were measured with a PTR-TOF-MS (Ionicon Analytik, TOF 1000 ultra). Trace gases (O_3 and NO_x) were measured with Instruments of Teledyne Technologies Inc. T400 and T200 at ECUST, Shanghai and with Thermo Fisher Scientific, TEI 49i and 42i equipped with BLC converter at SORPES, Nanjing (Xu et al., 2017). The OA was measured by TOF-ACSM at ECUST. The OA at SORPES was obtained from OC concentration. The detailed calibration and correction methods are described in Text S1 (supporting information).

3. Results and Discussion

The two observational sites are under influence of biogenic and anthropogenic interaction. The SORPES station is strongly affected by local biogenic and anthropogenic emissions. As is shown in Figures 1a and 1b, isoprene concentration showed a clear diurnal variation following solar radiation, with the averaged daytime concentration of over 2 ppb; NO concentration peaked during 06:00-10:00 LT indicating the effect of morning rush hour. Such effect of local biogenic emissions on ECUST, Shanghai was much weaker as is shown in Figure 1c. The NO_x concentration at ECUST was comparable with SORPES (Figures 1b and 1d). The mean NO_x concentration was 4.91 and 5.95 ppb at SORPES and ECUST during the observation period, respectively. The high NO_x concentration observed at both sites indicated high regional background of NO_x in eastern China. The daytime MVK + MACR/isoprene ratio at SORPES and ECUST ranged between 1.41–1.55 and 0.45–3.33, respectively. The high ratio indicated that under high-NO_x condition, isoprene hydroxy peroxy radicals (ISOPOO) + NO reaction likely dominated the fate of ISOPOO. The reacted isoprene concentration was estimated based on the in situ isoprene, MVK, and MACR concentration (Text S1, supporting information). On average, 45%–69% of isoprene was reacted during photochemical processes at SORPES. This value was comparable with the reported result in Beijing (Xie et al., 2008) and lower than 47%–90% at ECUST.

The higher ratio of reacted isoprene at ECUST indicated longer OH exposure after isoprene were emitted into atmosphere.

Strong biogenic and anthropogenic interaction occurred at the ECUST, Shanghai, only under favorable meteorological conditions. Long-term air mass trajectory analysis (Figure S5a) indicated a significant influence of biogenic emission from the south (35% of summer days during 2013–2018). During the period of the campaign (May 17 to June 27), the average isoprene concentration was three times higher when air masses were transported from southern forested areas (Figure S6). Field observation periods available with CIMS measurement at the two sites were shown in Figures S3 and S7, respectively. During the ECUST campaign, we captured one case that OA increased and accumulated synchronously with the increase in isoprene concentration (June 25 to 26). This case (see Text S2, in the supporting information, for details), along with the continuous observational results at the SORPES station, was discussed in the following sections.

3.1. Identification of Isoprene Multifunctional Products

To identify the isoprene multifunctional products or isoprene oxidized organic molecules (abbreviated as IPOOMs), an identification workflow was developed and performed on all identified compounds measured by CIMS. The characteristics of the molecular carbon number (nC), hydrogen number (nH), and effective oxygen number (nO, representing the actually oxygen number bonded with carbon molecules, nO = nO* − 2*(nN), where nO* denoted the original oxygen number) and molecular unsaturation degree (SD = nC + 1 − (nN + nH)/2) of IPOOMs were summarized based on the latest isoprene oxidation scheme (Wennberg et al., 2018) and performed to narrow down the pool of IPOOMs. Correlation analysis with $C_5H_{10}N_2O_8$ concentration and external tracers (e.g., concentration of isoprene, MVK + MACR, estimated OH radical) was then applied to further exclude compounds that were irrelevant or contradictious with variation of precursors. In general, we identified IPOOMs based on the following steps: (1) NO_3^--attached closed-shell molecules were selected; (2) molecules with nC = 4 and 5 were selected; (3) C4 compounds with SD range of 1–2, nO <=6, nH> = 6 and C5 compounds with SD range of 0–2, nO <=7, nH> = 8 were selected. The detailed descriptions about the workflow is provided in Text S3 (supporting information).

The NO_3^- CIMS measurements indicated that $C_5H_{10}N_2O_8$ showed the highest signal in counts per second among all observed compounds (9.4% and 7.5% at SORPES and ECUST) and that C4 and C5 oxidized compounds contributed over 15% to the total signal at both sites (Table S2). The signal intensity of C7 compounds at the SORPES were much larger than at the ECUST, which is attributed to higher concentration of aromatic precursors (toluene) at SORPES, Nanjing (Figure S8). Referring to the latest study of isoprene oxidation (Wennberg et al., 2018 and Schwantes et al., 2019), $C_5H_{10}N_2O_8$ was most likely to be isoprene dihydroxy dinitrates, second-generation oxidation products from OH initiated isoprene oxidation reactions in the presence of NO. The formation pathway of $C_5H_{10}N_2O_8$ is shown in Figures S9–S11: the reaction of OH with isoprene in the atmosphere proceeds mainly via OH addition to the C=C bond, leading to the formation of ISOPOO radicals (mostly 1,2-ISOPOO and 4,3-ISOPOO). The ISOPOO radicals react with NO to form isoprene hydroxyl nitrates (IHNs) via NO addition. Following addition of OH to the remaining double bond of IHNs, hydroxyl nitrooxy peroxy radical isomers are formed via addition of oxygen. The hydroxyl nitrooxy peroxy radical isomers react with NO to form isoprene dihydroxyl dinitrates, which contribute to the $m/z = 288$ signals measured by NO_3^- CIMS. $C_5H_{10}N_2O_8$ was reported as an isoprene nitrates and showed good correlation with sulfate and SO_2 at a forest site (Massoli et al., 2018). The formation of $C_5H_{10}N_2O_8$ is a strong indication of chemical interaction between both biogenic and anthropogenic emissions. The diel cycle of $C_5H_{10}N_2O_8$ (Figure 2a) shows a first peak at ~10:00 LT (local time) and a second but smaller increase at ~21:00 LT. This diel pattern was in consistence with the pattern of other reported functionalized nitrates (Lee et al., 2015; Xiong et al., 2015; Massoli et al., 2018). The normalized diel cycles of the most abundant isoprene oxidation products, including $C_5H_{8,10}N_2O_8$, $C_4H_7NO_6$, $C_5H_{7,9,11}NO_6$, $C_5H_{7,9}NO_7$, are shown in Figure 2b. Since OH radical is needed to initiate the reactions, all of functionalized compounds have day time peaks between 9:00–12:00 LT. It should also be noted that nighttime enhancement was also observed during 18:00-23:00 LT. There was sufficient O_3 and NO_2 during that period ($[O_3]$ ≈40 ppb; $[NO_2]$≈5 ppb), promoting NO_3 production. NO_3 involved reactions could contribute to the nighttime enhancement of IPOOMs. Substantial unsaturated C5 dinitrates ($C_5H_8N_2O_8$), consisting of 8.89% of total mole concentration of identified

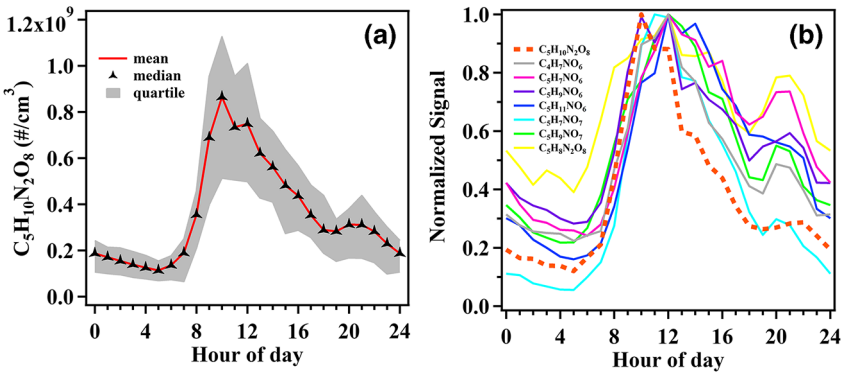

Figure 2. (a) Diel pattern of isoprene dihydroxyl dinitrates ($C_5H_{10}N_2O_8$) and (b) Normalized diel pattern of the most abundant isoprene multifunctional products identified at SORPES, Nanjing.

IPOOMs, were observed during the case at ECUST, Shanghai. Experimental results were supportive that $C_5H_8N_2O_8$ and $C_5H_{10}N_2O_8$ can be produced in NO_3+ isoprene system (Ng et al., 2008); while, to our knowledge, there was no relevant reports from field observations.

3.2. Characteristics of IPOOMs

Characteristics of identified IPOOMs were statistically analyzed according to different criteria (Figures 3 and S12). It should be noted that NO_3^- CIMS was insensitive to the compounds with O/C ratio lower than 0.6–0.7 (Simon et al., 2020; Stolzenburg et al., 2018), the statistical analysis would underestimate the contribution of less oxidized organics. The most abundant IPOOMs were given in pie chart (Figure 3a), representing the relative contributions of individual IPOOM to the total mole concentration of IPOOMs. Compared with composition of isoprene functionalized products under low-NO condition (Krechmer et al., 2015), formation of hydroperoxides was suppressed and isoprene RO_2 + NO reactions dominated the fate of isoprene oxidation due to the observed high-NO_x concentration. Supportive evidence can also be addressed from high MVK + MACR/isoprene ratio observed during summer time (in the range of 0.45–3.33). Although considering as a minor path from isoprene RO_2 + NO reactions, organic nitrates constitute large proportion of IPOOM composition: 72% of IPOOMs mole concentration were identified as nitrogen-containing species; 42% of IPOOMs mole concentration were identified as dinitrates, and $C_5H_{10}N_2O_8$ alone contributed about 85% of dinitrate mole concentration (Figure 3b). NO_3 oxidation reactions were also an important source of isoprene organic nitrate, since we can observe tri-nitrates even during daytime. The proportion of tri-nitrates increased to about 3% of total IPOOMs mole concentration during early night at SORPES, Nanjing when radiation condition was weakened and there was still plenty of isoprene in the air indicating that NO_3 chemistry during early night was an important sink of NO_x (Figure S13). The PMF analysis on oxidized organics at SORPES have separated one isoprene NO_3 factor. The representative compounds of this factor were $C_5H_{10}N_2O_8$ and $C_5H_9N_3O_{10}$. $C_5H_9N_3O_{10}$ was supposed to be isoprene hydroxyl tri-nitrates, which can only be form through NO_3 oxidation (see details in Text S4, supporting information).

The highest contribution came from IPOOMs with nO = 4 and 5, constituting of 89% IPOOM mole concentration (Figure 3c). The fact that NO_3^- CIMS is more sensitive to highly oxygenated molecules (Ehn et al., 2014; Yan et al., 2016) suggests that the observed distribution of IPOOMs with nO = 6 and 7 accounts for less than 5% of total IPOOMs mole concentration was not due to instrument sensitivity. Such decreasing trend with increasing nO in gas phase was also reported by Lee et al. (2015). This decreasing trend can be explained by the high regional NOx concentration and the decreased volatility with increasing oxidation state.

The distribution of IPOOMs SD is shown in Figure 3d, saturated functionalized compound constituted 44% of IPOOMs mole concentration, unsaturated functionalized with SD = 1 and 2 constituted 34% and 22% of IPOOMs mole concentration, respectively. Such distribution indicated that within the selectivity range of NO_3^- CIMS, more IHNs and hydroxyl hydroperoxides were observed than isoprene carbonyls and di-carbonyls.

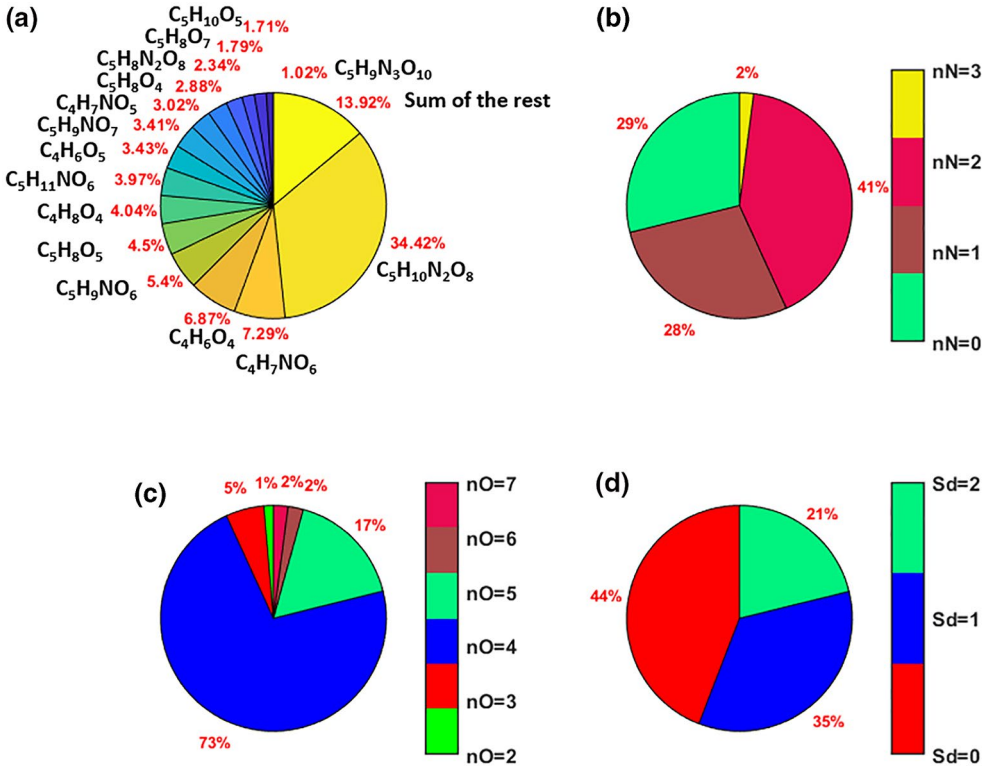

Figure 3. Relative concentration of averaged daytime (LT 10:00-14:00) IPOOMs concentration at the SORPES, Nanjing according to different statistical criteria: (a) Different IPOOMs composition; (b) IPOOMs containing different nitrate groups; (c) IPOOMs containing different oxygen number; (d) IPOOMs with different molecular saturation degree. This statistical result only reflected the distribution of organic molecules within the selectivity of NO_3^- CIMS. CIMS, chemical ionization mass spectrometer.

To evaluate the contribution of IPOOMs to SOA, we calculated the saturation vapor pressures of the detected IPOOMs. The determination of IPOOM molecular structures is not possible with the available data, which made a more precise and structure-based volatility estimation difficult to apply. Consequently, the group-contribution method was applied for this analysis, using the molecular bulk properties to parametrize the volatility of each IPOOM at 300 K (also listed in Table S3). The volatility estimation reflected that over 98% of IPOOMs by mole were categorized as semi-VOC (SVOC) and intermediate-VOC (IVOC), volatility (logarithm of saturation mass concentration) ranging from −0.5 to −5, while only 1.3% of IPOOMs by mole were categorized as low-VOC (LVOC) (Figure 4a). The volatility distribution indicated that, under high-NO_x concentration, the functionalized products tend to be more volatile (73% of total mole concentration were O_4 compounds), compared with hydroxy dihydroperoxides ($C_5H_{10}O_{5\text{-}6}$) being the main functionalized products under low-NO condition (Krechmer et al., 2015).

3.3. Estimation of Particle-Phase Contribution

Condensation of IPOOMs to OA was evaluated based on the equilibrium partitioning between gas and particle phase (method described in Text S5, supporting information). Uncertainties about OA contribution were mainly introduced by two factors: (1) volatility estimation that affected partitioning coefficient and (2) IPOOM calibration that affected IPOOM concentration. The volatility estimated by group-contribution method was compared with those reported by Schwantes et al. (2019). In general, the differences of volatilities were within an order of magnitude and the group-contribution method tended to overestimate the volatilities of SVOCs by a factor of 3–5. For example, $C_5H_{10}N_2O_8$ (isoprene dihydroxyl dinitrates) has the saturation mass concentration of 33.8 $\mu g/m^3$ at 300 K calculated from the group-contribution method. The calculated saturation mass concentration of isoprene 1,3-dihydroxyl 2,4-dinitrate, isoprene 2,4-dihydroxyl

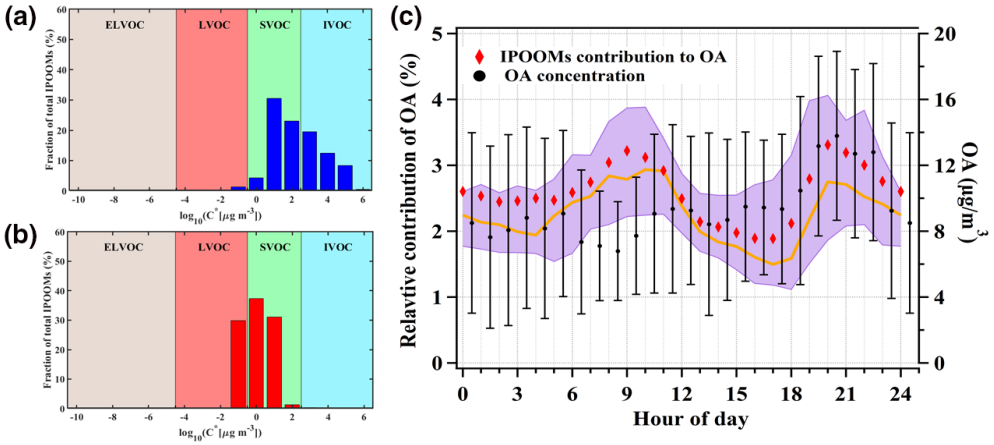

Figure 4. (a) Volatility distribution of IPOOMs at 300 K, IPOOMs were grouped in bins separated by an order of magnitude in C* and normalized by the total concentration of IPOOMs; (b) same plot as panel (a), with normalized particle-phase concentration; (c) diel cycle of IPOOMs relative contribution to OA, averaged from observation period (red diamond represent mean value, solid line represent median value, and shading areas represent 25% and 75% percentile) and observed OA concentration with standard deviation (black dots with error bars).

1,3-dinitrate, and isoprene 1,4-dihydroxyl 2,3-dinitrate is 7.67, 13.2, and 5.23 μg/m^3. It should be noted that the difference of volatility cannot reflect the real situation of bulk volatility estimation, since the contribution of different isomers is unknown. The uncertainty of the volatility of individual IPOOM as well as the overall volatility distribution is hard to get, the current estimation is based on our best knowledge and established methods (Mohr et al., 2019; Simon et al., 2020; Stolzenburg et al., 2018; Yan et al., 2020). An additional 33% uncertainty is also introduced from the determination of the calibration factor of IPOOMs (Kürten et al., 2012). The average mass of total condensed IPOOMs at two observational sites was 0.28 ± 0.27 μg/m^3, accounting for 2.6% of the total OA (error bonds represent the standard deviation). The relative contribution to particle-phase IPOOMs is shown in Figure 4b. Although, constitute only 1.3% of total gas-phase IPOOMs concentration, LVOC contributed 29.9% of particle-phase concentration. SVOC contributed to 70.1% of particle-phase concentration. To investigate the relative contribution of different isoprene SOA, IEPOX-SOA contribution in ECUST was resolved with a-value PMF (Text S6, supporting information), the average concentration was 0.24 μg/m^3, accounting for 2.3% of total OA. The result showed that IEPOX-SOA were significantly lower than the reported concentration by various field campaigns with relatively lower NO concentration, which account for 6%–36% of total OA (Budisulistiorini et al., 2013; Hu et al., 2015); but were comparable with the IEPOX-SOA (0.33 ± 0.19 μg/m^3, 3.8% of the total OA) reported in Nanjing at 2013 summer (Zhang et al., 2017). The filter-based analysis had also indicated that IEPOX-SOA formation was significantly suppressed in China due to high-NO_x concentration (Ding et al., 2016). In ECUST, the contribution of isoprene SOA (IEPOX-SOA + IPOOM condensation) accounted for 4.3% (2.9%–6.1%) of total OA (0.73 ± 0.27 μg/m^3, average ± standard deviation) during the reported episode. The estimated IPOOM condensation showed good correlation with IEPOX-SOA ($R^2 = 0.79$) and their contribution was comparable (Figure S21). It should also be noted that the reactive uptake by preexisting aerosol and subsequent hydrolysis might be another important pathway of isoprene SOA formation from IPOOMs under high humidity and aerosol water content conditions during summer. The hydrolysis of IHN to form diols and nitric acid has been proposed by Jacob et al. (2014); but the hydrolysis rate of functionalized isoprene nitrates is poorly studied yet and need further study. Thus, the contribution of IPOOMs to SOA in polluted regions, such as eastern China, was comparable or even higher than IEPOX channel and the sources of isoprene SOA need to be re-evaluated in polluted regions.

The modeled results further indicated that the relative contribution of IPOOMs is highest during two periods, which were around 10:00 LT and 20:00 LT (Figure 4c). The daytime peak was consistent with the high concentration of IPOOMs, while the night time peak was attributed to the integrated influence of OA concentration, temperature, and IPOOM concentration. The increased OA concentration led to higher parti-

tioning coefficient; the decreased temperature led to the decrease of volatility promoting the condensation; the nighttime formation occurred at this time period for IPOOMs provided more gas-phase precursors than afternoon and dusk. The functionalized organic nitrates dominant the total mole concentration of identified IPOOMs in Shanghai and Nanjing, accounting for 72% and 88%, respectively. Although $C_5H_{10}N_2O_8$ constituted of large proportion of gas-phase IPOOMs concentration, more oxidized functionalized nitrates were also important in particle phase (Figure S22). It should also be noted that NO_3^- CIMS is less sensitive to less oxidized organic compounds (Figure 3c). Although these compounds are likely categorized as IVOC, their contribution on OA should not be neglected when OA concentration is sufficient. Thus, our estimated OA contribution should be considered as a lower limit.

4. Conclusions

Simultaneous ground measurements of gas-phase precursors, oxidized organic compounds, and OA were conducted at two suburban sites located in east China during 2018 summer. Isoprene oxidized organic compounds (IPOOMs) were identified to contribute large fraction of NO_3^- CIMS signal, of which isoprene dihydroxyl dinitrate ($C_5H_{10}N_2O_8$) showed the highest concentration at both sites. The observational results indicated that in the atmosphere with high NO_x and isoprene concentration: (1) RO_2-NO reactions dominate the fate of isoprene oxidation (likely the same for other VOC oxidation); (2) multigeneration oxidation reactions are important, supported by the high concentration of saturated IPOOMs. Most of the IPOOMs were SVOC and contributed to 2.6% of the total OA through gas/particle partitioning. Further study is necessary to obtain a more quantitative observation of particle phase functionalized organic composition and to estimate large-scale contribution of functionalized organic compounds to SOA formation in polluted regions.

Data Availability Statement

The measurement data used is available at ZENODO (https://zenodo.org, https://doi.org/10.5281/zenodo.3901111).

Acknowledgments
The research was supported by National Key Research & Development Program of China (2016YFC0200500 and 2016YFC0202000) and National Science Foundation of China (41675145, 41725020, 91544231, 91644218, 41422504, 91744311, 41875175 and 42005086). The authors thank Dr. Zhou Lei and Mr. Yan Lei from School of Resources and Environmental Engineering, East China University of Science and Technology for their help with the campaign.

References

Bates, K. H., Crounse, J. D., St. Clair, J. M., Bennett, N. B., Nguyen, T. B., Seinfeld, J. H., et al. (2014). Gas phase production and loss of isoprene epoxydiols. *The Journal of Physical Chemistry. A*, *118*, 1237–1246.

Bates, K. H., & Jacob, D. J. (2019). A new model mechanism for atmospheric oxidation of isoprene: Global effects on oxidants, nitrogen oxides, organic products, and secondary organic aerosol. *Atmospheric Chemistry and Physics*, *19*(14), 9613–9640. https://doi.org/10.5194/acp-19-9613-2019

Berndt, T., Herrmann, H., Sipilä, M., & Kulmala, M. (2016). Highly oxidized second-generation products from the gas-phase Reaction of OH radicals with isoprene. *The Journal of Physical Chemistry. A*, *120*(51), 10150–10159. https://doi.org/10.1021/acs.jpca.6b10987

Budisulistiorini, S. H., Canagaratna, M. R., Croteau, P. L., Marth, W. J., Baumann, K., Edgerton, E. S., et al. (2013). Real-time continuous characterization of secondary organic aerosol derived from isoprene epoxydiols in downtown Atlanta, Georgia, using the Aerodyne Aerosol Chemical Speciation Monitor. *Environmental Science & Technology*, *47*(11), 5686–5694. https://doi.org/10.1021/es400023n

Carlton, A. G., Wiedinmyer, C., & Kroll, J. H. (2009). A review of Secondary Organic Aerosol (SOA) formation from isoprene. *Atmospheric Chemistry & Physics*, *9*(14), 4987–5005. https://doi.org/10.5194/acpd-9-8261-2009

Chan, A. W. H., Chan, M. N., Surratt, J. D., Chhabra, P. S., Loza, C. L., Crounse, J. D., et al. (2010). Role of aldehyde chemistry and NOx concentrations in secondary organic aerosol formation. *Atmospheric Chemistry and Physics*, *10*(15), 7169–7188. https://doi.org/10.5194/acp-10-7169-2010

Claeys, M., Graham, B., Vas, G., Wang, W., Vermeylen, R., Pashynska, V., et al. (2004). Formation of secondary organic aerosols through photooxidation of isoprene. *Science*, *303*(5661), 1173–1176. https://doi.org/10.1126/science.1092805

Ding, A. J., Fu, C. B., Yang, X. Q., Sun, J. N., Zheng, L. F., Xie, Y. N., et al. (2013). Ozone and fine particle in the western Yangtze River Delta: An overview of 1 yr data at the SORPES station. *Atmospheric Chemistry and Physics*, *13*(11), 5813–5830. https://doi.org/10.5194/acp-13-5813-2013

Ding, X., He, Q. F., Shen, R. Q., Yu, Q. Q., Zhang, Y. Q., Xin, J. Y., et al. (2016). Spatial and seasonal variations of isoprene secondary organic aerosol in China: Significant impact of biomass burning during winter. *Scientific Reports*, *6*, 20411. https://doi.org/10.1038/srep20411

Dommen, J., Metzger, A., Duplissy, J., Kalberer, M., Alfarra, M. R., Gascho, A., et al. (2006). Laboratory observation of oligomers in the aerosol from isoprene/NOx photooxidation. *Geophysical Research Letters*, *33*(13), 805–809. https://doi.org/10.1029/2006gl026523

D'Ambro, E. L., Lee, B. H., Liu, J., Shilling, J. E., Gaston, C. J., Lopez-Hilfiker, F. D., et al. (2017). Molecular composition and volatility of isoprene photochemical oxidation secondary organic aerosol under low- and high-NOx conditions. *Atmospheric Chemistry and Physics*, *17*(1), 159–174. https://doi.org/10.5194/acp-17-159-2017

Ehn, M., Thornton, J. A., Kleist, E., Sipila, M., Junninen, H., & Pullinen, I. (2014). A large source of low-volatility secondary organic aerosol. *Nature*, *506*, 476–479. https://doi.org/10.1038/nature13032

Guenther, A., Karl, T., Harley, P., Wiedinmyer, C., Palmer, P. I., & Geron, C. (2006). Estimates of global terrestrial isoprene emissions using MEGAN (Model of Emissions of Gases and Aerosols from Nature). *Atmospheric Chemistry and Physics*, *6*, 3181–3210. http://www.atmos-chem-phys.net/6/3181/2006/

Huang, R. J., Zhang, Y., Bozzetti, C., Ho, K. F., Cao, J. J., Han, Y., et al. (2014). High secondary aerosol contribution to particulate pollution during haze events in China. *Nature*, *514*(7521), 218–222. https://doi.org/10.1038/nature13774

Hu, W. W., Campuzano-Jost, P., Palm, B. B., Day, D. A., Ortega, A. M., Hayes, P. L., et al. (2015). Characterization of a real-time tracer for isoprene epoxydiols-derived secondary organic aerosol (IEPOX-SOA) from aerosol mass spectrometer measurements. *Atmospheric Chemistry and Physics*, *15*(20), 11807–11833. https://doi.org/10.5194/acp-15-11807-2015

Jacobs, M. I., Burke, W. J., & Elrod, M. J. (2014). Kinetics of the reactions of isoprene-derived hydroxynitrates: Gas phase epoxide formation and solution phase hydrolysis. *Atmospheric Chemistry and Physics*, *14*(17), 8933–8946. https://doi.org/10.5194/acp-14-8933-2014

Kjaergaard, H. G., Knap, H. C., Ørnsø, K. B., Jørgensen, S., Crounse, J. D., Paulot, F., & Wennberg, P. O. (2012). Atmospheric fate of methacrolein. 2. Formation of lactone and implications for organic aerosol production. *The Journal of Physical Chemistry A*, *116*(24), 5763–5768. https://doi.org/10.1021/jp210853h

Krechmer, J. E., Coggon, M. M., Massoli, P., Nguyen, T. B., Crounse, J. D., Hu, W., et al. (2015). Formation of low volatility organic compounds and secondary organic aerosol from isoprene hydroxyhydroperoxide low-NO oxidation. *Environmental Science & Technology*, *49*(17), 10330–10339. https://doi.org/10.1021/acs.est.5b02031

Kroll, J. H., Nga, L. N., Murphy, S. M., Flagan, R. C., & Seinfeld, J. H. (2006). Secondary organic aerosol formation from isoprene photooxidation. *Environmental Science & Technology*, *40*(6), 1869–1877. https://doi.org/10.1021/es0524301

Kroll, J. H., Ng, N. L., Murphy, S. M., Flagan, R. C., & Seinfeld, J. H. (2005). Secondary organic aerosol formation from isoprene photooxidation under high-NOx conditions. *Geophysical Research Letters*, *32*(18), 808–811. https://doi.org/10.1029/2005gl023637

Kroll, J. H., & Seinfeld, J. H. (2008). Chemistry of secondary organic aerosol: Formation and evolution of low-volatility organics in the atmosphere. *Atmospheric Environment*, *42*(16), 3593–3624. https://doi.org/10.1016/j.atmosenv.2008.01.003

Kurten, A., Rondo, L., Ehrhart, S., & Curtius, J. (2012). Calibration of a chemical ionization mass spectrometer for the measurement of gaseous sulfuric acid. *The Journal of Physical Chemistry A*, *116*(24), 6375–6386. https://doi.org/10.1021/jp212123n

Lee, B., Mohr, H. C., Lopez-Hilfiker, F. D., Lutz, A., Hallquist, M., & Lee, L. (2015). Highly functionalized organic nitrates in the southeast United States: Contribution to secondary organic aerosol and reactive nitrogen budgets. *Proceedings of the National Academy of Sciences of the United States of America*, *113*(6), 1516–1521. https://doi.org/10.1073/pnas.1508108113

Lee, L., Teng, A. P., Wennberg, P. O., Crounse, J. D., & Cohen, R. C. (2014). On rates and mechanisms of OH and O_3 reactions with isoprene-derived hydroxy nitrates. *The Journal of Physical Chemistry A*, *118*(9), 1622–1637. https://doi.org/10.1021/jp4107603

Lin, Y.-H., Zhang, Z., Docherty, K. S., Zhang, H., Budisulistiorini, S. H., Rubitschun, C. L., et al. (2011). Isoprene epoxydiols as precursors to secondary organic aerosol formation: Acid-catalyzed reactive uptake studies with authentic compounds. *Environmental Science & Technology*, *46*(1), 250–258. https://doi.org/10.1021/es202554c

Lin, Y.-H., Zhang, H., Pye, H. O., Zhang, Z., Marth, W. J., Park, S., et al. (2013). Epoxide as a precursor to secondary organic aerosol formation from isoprene photooxidation in the presence of nitrogen oxides. *Proceedings of the National Academy of Sciences of the United States of America*, *110*(17), 6718–6723.

Liu, J., D'Ambro, E. L., Lee, B. H., Lopez-Hilfiker, F. D., Zaveri, R. A., Rivera-Rios, J. C., et al (2016). Efficient isoprene secondary organic aerosol formation from a non-IEPOX pathway. *Environmental Science & Technology*, *50*(18), 9872–9880. https://doi.org/10.1021/acs.est.6b01872

Liu, Y., Kuwata, M., Strick, B. F., Geiger, F. M., Thomson, R. J., McKinney, K. A., et al. (2015). Uptake of epoxydiol isomers accounts for half of the particle-phase material produced from isoprene photooxidation via the HO_2 pathway. *Environmental Science & Technology*, *49*(1), 250–258. https://doi.org/10.1021/es5034298

Massoli, P., Stark, H., Canagaratna, M. R., Krechmer, J. E., Xu, L., Ng, N. L., et al. (2018). Ambient measurements of highly oxidized gas-phase molecules during the southern oxidant and aerosol study (SOAS) 2013. *ACS Earth and Space Chemistry*, *2*(7), 653–672. https://doi.org/10.1021/acsearthspacechem.8b00028

Mohr, C., Thornton, J. A., Heitto, A., Lopez-Hilfiker, F. D., Lutz, A., Riipinen, I., et al. (2019). Molecular identification of organic vapors driving atmospheric nanoparticle growth. *Nat Commun*, *10*(1), 4442. https://doi.org/10.1038/s41467-019-12473-2

Müller, J.-F., Stavrakou, T., & Peeters, J. (2019). Chemistry and deposition in the Model of Atmospheric composition at Global and Regional scales using Inversion Techniques for Trace gas Emissions (MAGRITTE v1.1) – Part 1: Chemical mechanism. *Geoscientific Model Development*, *12*, 2307–2356. https://doi.org/10.5194/gmd-12-2307-2019

Ng, N. L., Canagaratna, M. R., Zhang, Q., Jimenez, J. L., Tian, J., Ulbrich, I. M., et al. (2010). Organic aerosol components observed in Northern Hemispheric datasets from Aerosol Mass Spectrometry. *Atmospheric Chemistry and Physics*, *10*(10), 4625–4641. https://doi.org/10.5194/acp-10-4625-2010

Ng, N. L., Kroll, J. H., Keywood, M. D., Bahreini, R., Varutbangkul, V., Flagan, R. C., & Seinfeld, J. H. (2006). Contribution of first – versus second-generation products to secondary organic aerosols form in the oxidation of biogenic hydrocarbons. *Environmental Science & Technology*, *40*(7), 2283–2297. https://doi.org/10.1021/es052269u

Ng, N. L., Kwan, A. J., Surratt, J. D., Chan, A. W. H., Chhabra, P. S., Sorooshian, A., et al. (2008). Secondary Organic Aerosol (SOA) formation from reaction of isoprene with nitrate radicals (NO_3). *Atmospheric Chemistry and Physics*, *8*, 4117–4140. https://doi.org/10.5194/acp-8-4117-2008

Nguyen, T. B., Coggon, M. M., Bates, K. H., Zhang, X., Schwantes, R. H., Schilling, K. A., et al. (2014). Organic aerosol formation from the reactive uptake of isoprene epoxydiols (IEPOX) onto non-acidified inorganic seeds. *Atmospheric Chemistry and Physics*, *14*(7), 3497–3510. https://doi.org/10.5194/acp-14-3497-2014

Nguyen, T. B., Kelvin, H. B., Crounse, J. D., Schwantes, R. H., Zhang, X., Kjaergaard, H. G., et al. (2015). Mechanism of the hydroxyl radical oxidation of methacryloyl peroxynitrate (MPAN) and its pathway toward secondary organic aerosol formation in the atmosphere. *Physical Chemistry Chemical Physics*, *17*(27), 17914–17926. https://doi.org/10.1039/c5cp02001h

Pai, S. J., Heald, C. L., Pierce, J. R., Farina, S. C., Marais, E. A., Jimenez, J. L., et al. (2020). An evaluation of global organic aerosol schemes using airborne observations. *Atmospheric Chemistry and Physics*, *20*(5), 2637–2665. https://doi.org/10.5194/acp-20-2637-2020

Paulot, F., Crounse, J. D., Kjaergaard, H. G., Kürten, A., St. Clair, J. M., Seinfeld, J. H., & Wennberg, P. O. (2009). Unexpected epoxide formation in the gas-phase photooxidation of isoprene. *Science*, *325*(5941), 730–733. https://doi.org/10.1126/science.1172910

Qi, X. M., Ding, A. J., Nie, W., Chi, X. G., Huang, X., Xu, Z., et al. (2019). Direct measurement of new particle formation based on tethered airship around the top of the planetary boundary layer in eastern China. *Atmospheric Environment*, *209*, 92–101. https://doi.org/10.1016/j.atmosenv.2019.04.024

Riva, M., Budisulistiorini, S. H., Chen, Y. Z., Zhang, Z. F., D'Ambro, E. L., Zhang, X., et al. (2016). Chemical characterization of secondary organic aerosol from oxidation of isoprene hydroxyhydroperoxides. *Environmental Science & Technology*, *50*(18), 9889–9899. https://doi.org/10.1021/acs.est.6b02511

Schwantes, R. H., Charan, S. M., Bates, K. H., Huang, Y., Nguyen, T. B., Mai, H., et al. (2019). Low-volatility compounds contribute significantly to isoprene SOA under high-NOx conditions. *Atmospheric Chemistry and Physics*, *19*(11), 7255–7278. https://doi.org/10.5194/acp-19-7255-2019

Setyan, A., Zhang, Q., Merkel, M., Knighton, W. B., Sun, Y., Song, C., et al. (2012). Characterization of submicron particles influenced by mixed biogenic and anthropogenic emissions using high-resolution aerosol mass spectrometry: Results from CARES. *Atmospheric Chemistry and Physics*, *12*(17), 8131–8156. https://doi.org/10.5194/acp-12-8131-2012

Shilling, J. E., Zaveri, R. A., Fast, J. D., Kleinman, L., Alexander, M. L., Canagaratna, M. R., et al. (2013). Enhanced SOA formation from mixed anthropogenic and biogenic emissions during the CARES campaign. *Atmospheric Chemistry and Physics*, *13*(4), 2091–2113. https://doi.org/10.5194/acp-13-2091-2013

Simon, M., DaDa, L., Heinritzi, M., Scholz, W., Stolzenburg, D., Fischer, L., et al. (2020). Molecular understanding of new-particle formation from α-pinene between −50 and +25°C. *Atmospheric Chemistry and Physics*, *20*(15), 9183–9207. https://doi.org/10.5194/acp-2019-1058

Stadtler, S., Kühn, T., Schröder, S., Taraborrelli, D., Schultz, M. G., & Kokkola, H. (2018). Isoprene-derived secondary organic aerosol in the global aerosol-chemistry-climate model ECHAM6.3.0-HAM2.3-MOZ1.0. *Geoscientific Model Development*, *11*, 3235–3260. https://doi.org/10.5194/gmd-11-3235-2018

Stolzenburg, D., Fischer, L., Vogel, A. L., Heinritzi, M., Schervish, M., Simon, M., et al. (2018). Rapid growth of organic aerosol nanoparticles over a wide tropospheric temperature range. *Proceedings of the National Academy of Sciences of the United States of America*, *115*(37), 9122–9127. https://doi.org/10.1073/pnas.1807604115

Sun, Y. L., Wang, Z. F., Fu, P. Q., Yang, T., Jiang, Q., Dong, H. B., et al. (2013). Aerosol composition, sources and processes during wintertime in Beijing, China. *Atmospheric Chemistry and Physics*, *13*, 4577–4592. https://doi.org/10.5194/acp-13-4577-2013

Surratt, J. D., Chan, A. W. H., Eddingsaas, N. C., Chan, M., Loza, C. L., Kwan, A. J., et al. (2009). Reactive intermediates revealed in secondary organic aerosol formation from isoprene. *Proceedings of the National Academy of Sciences of the United States of America*, *107*(15), 6640–6645. https://doi.org/10.1073/pnas.0911114107

Wang, S., Riva, M., Yan, C., Ehn, M., Wang, L. M., et al (2018). Primary formation of highly oxidized multifunctional products in the OH-initiated oxidation of isoprene: A combined theoretical and experimental study. *Environmental Science & Technology*, *52*(21), 12255–12264. https://doi.org/10.1021/acs.est.8b02783

Wennberg, P. O., Bates, K. H., Crounse, J. D., Dodson, L. G., McVay, R. C., Mertens, L. A., et al. (2018). Gas-phase reactions of isoprene and its major oxidation products. *Chemical Reviews*, *118*(7), 3337–3390. https://doi.org/10.1021/acs.chemrev.7b00439

Xie, X., Shao, M., Liu, Y., Lu, S., Chang, C., & Chen, Z. (2008). Estimate of initial isoprene contribution to ozone formation potential in Beijing, China. *Atmospheric Environment*, *42*(24), 6000–6010. https://doi.org/10.1016/j.atmosenv.2008.03.035

Xiong, F., Teng, A., Wennberg, P., Crounse, J. D., Nguyen, T. B., et al. (2015). Observation of isoprene hydroxynitrates in the southeastern United States and implications for the fate of NOx. *Atmospheric Chemistry and Physics*, *15*(19), 11257–11272. https://doi.org/10.5194/acp-15-11257-2015

Xu, L., Guo, H., Boyd, C. M., Klein, M., Bougiatioti, A., Cerully, K. M., et al. (2015). Effects of anthropogenic emissions on aerosol formation from isoprene and monoterpenes in the southeastern United States. *Proceedings of the National Academy of Sciences of the United States of America*, *112*(1), 37–42. https://doi.org/10.1073/pnas.1417609112

Xu, Z. N., Huang, X., Nie, W., Chi, X. G., Xu, Z., & Zheng, L. F. (2017). Influence of synoptic condition and holiday effects on VOCs and ozone production in the Yangtze River Delta region, China. *Atmospheric Environment*, *168*, 112–124. https://doi.org/10.1016/j.atmosenv.2017.08.035

Xu, L., Kollman, M. S., Song, C., Shilling, J. E., & Ng, N. L. (2014). Effects of NOx on the volatility of secondary organic aerosol from isoprene photooxidation. *Environmental Science & Technology*, *48*(4), 2253–2262. https://doi.org/10.1073/pnas.1417609112

Yan, C., Nie, W., Äijälä, M., Rissanen, M. P., Canagaratna, M. R., Massoli, P., & Junninen, H. (2016). Source characterization of highly oxidized multifunctional compounds in a boreal forest environment using positive matrix factorization. *Atmospheric Chemistry and Physics*, *16*(19), 12715–12731. https://doi.org/10.5194/acp-16-12715-2016

Yan, C., Nie, W., Vogel, A., Dada, L., Lehtipalo, K., Stolzenburg, D., et al. (2020). Size-dependent influence of NOx on the growth rates of organic aerosol particles. *Science Advances*, *6*(22), eaay4945. https://doi.org/10.1126/sciadv.aay4945

Zhang, Q., Jiménez, J., Coe, H., Ulbrich, I., Takami, A., Džepina, K., et al. (2007). Ubiquity and dominance of oxygenated species in organic aerosols in anthropogenically-influenced Northern Hemisphere midlatitudes. *Geophysical Research Letters*, *34*(13), L13801. https://doi.org/10.1029/2007GL029979

Zhang, Y., Tang, L., Sun, Y. L., Favez, O., Canonaco, F., Albinet, A., et al. (2017). Limited formation of isoprene epoxydiols-derived secondary organic aerosol under NOx-rich environments in Eastern China. *Geophysical Research Letters*, *44*(4), 2035–2043. https://doi.org/10.1002/2016GL072368

Zhang, H., Yee, L. D., Lee, B. H., Curtis, M. P., Worton, D. R., Isaacman-VanWertz, G., et al. (2018). Monoterpenes are the largest source of summertime organic aerosol in the southeastern United States. *Proceedings of the National Academy of Sciences of the United States of America*, *115*(9), 2038–2043. https://doi.org/10.1073/pnas.1717513115

Zhang, Y., Chen, Y. Z., Lambe, A., Olson, N. E., Lei, Z. Y., Craig, R. L., et al. (2018). Effect of the aerosol-phase state on secondary organic aerosol formation from the reactive uptake of iosprene-derived epoxydiols (IEPOX). *Environmental Science & Technology Letters*, *5*(3), 167–174. https://doi.org/10.1021/acs.estlett.8b00044

Zhang, H., Surratt, J. D., Lin, Y. H., Bapat, J., & Kamens, R. M. (2011). Effect of relative humidity on SOA formation from isoprene/NO photooxidation: Enhancement of 2-methylglyceric acid and its corresponding oligoesters under dry conditions. *Atmospheric Chemistry and Physics*, *11*(13), 6411–6424. https://doi.org/10.5194/acp-11-6411-2011

Reference From the Supporting Information

Donahue, N. M., Epstein, S. A., Pandis, S. N., & Robinson, A. L. (2011). A two-dimensional volatility basis set: 1. Organic-aerosol mixing thermodynamics. *Atmospheric Chemistry and Physics*, *11*(7), 3303–3318.